Submitted to Journal of the
Electrochemical Society

UCRL-19617
Preprint

c.2

RECEIVED
LAWRENCE
RADIATION LABORATORY

NOV 13 1970

LIBRARY AND
DOCUMENTS SECTION

CRYSTALLOGRAPHIC FACTORS IN HIGH-RATE ANODIC DISSOLUTION OF COPPER

D. Landolt, R. H. Muller,
and C. W. Tobias

September 1970

AEC Contract No. W-7405-eng-48

TWO-WEEK LOAN COPY

This is a Library Circulating Copy which may be borrowed for two weeks. For a personal retention copy, call Tech. Info. Division, Ext. 5545

LAWRENCE RADIATION LABORATORY
UNIVERSITY of CALIFORNIA BERKELEY

UCRL-19617 c.2

25

DISCLAIMER

This document was prepared as an account of work sponsored by the United States Government. While this document is believed to contain correct information, neither the United States Government nor any agency thereof, nor the Regents of the University of California, nor any of their employees, makes any warranty, express or implied, or assumes any legal responsibility for the accuracy, completeness, or usefulness of any information, apparatus, product, or process disclosed, or represents that its use would not infringe privately owned rights. Reference herein to any specific commercial product, process, or service by its trade name, trademark, manufacturer, or otherwise, does not necessarily constitute or imply its endorsement, recommendation, or favoring by the United States Government or any agency thereof, or the Regents of the University of California. The views and opinions of authors expressed herein do not necessarily state or reflect those of the United States Government or any agency thereof or the Regents of the University of California.

UCRL-19617

CRYSTALLOGRAPHIC FACTORS IN HIGH-RATE ANODIC DISSOLUTION OF COPPER

D. Landolt,* R. H. Muller and C. W. Tobias

Inorganic Materials Research Division, Lawrence Radiation Laboratory and Department of Chemical Engineering, University of California, Berkeley, California 94720

Abstract

Surface textures resulting from the anodic dissolution of polycrystalline and single crystal copper at 50 A/cm^2 in 2 M KNO_3 have been studied. Electrolyte flow velocities of 2500 and 400 cm/sec have been used for dissolution in the active and transpassive mode. Results obtained by light and electron microscopy show that surface topography resulting from active dissolution depends on crystal orientation. Flow streaks appear in transpassive dissolution. Transpassive pitting was observed in polycrystalline samples only.

* School of Engineering and Applied Science, University of California, Los Angeles, Calif. 90024.

An important problem in the process of electrochemical machining is the control of the resulting surface finish. In previous studies of high rate anodic metal dissolution (1-3), it has been shown that the surface finish resulting from the anodic dissolution of copper in a given electrolyte depends both on flow velocity and current density. The micrographs shown in Fig. 1 exhibit a transition from etching to polishing dissolution along a line running approximately from the upper left to the lower right of the array. Below this line, the surface appears etched and dull; above it, smooth and bright, with pits increasing in prominence with the separation from the transition region. The transition in surface finish coincides with the transition from a low voltage dissolution mode, which we have termed active, to a high voltage mode, which we call transpassive. It is to be expected that structural factors of the anode material also affect the resulting surface finish. In the present study, the surface topography resulting from the high-rate anodic dissolution of copper specimens has been investigated under active and transpassive dissolution conditions in 2 molar potassium nitrate solution. Polycrystalline samples of variable grain size and single crystals of different orientation have been used.

Experimental

The flow system and the electrical circuit employed have been described before.[1] Two flow rates have been employed, 2500 cm/sec for dissolution in the active mode and 400 cm/sec for dissolution in the passive mode. Electrolysis was conducted at constant current of 50 A/cm^2 with a stainless steel cathode of 3 mm diameter positioned 0.5 mm from the anode. During each experiment, a charge of 25 $coulombs/cm^2$ was

passed, which corresponds to an average dissolution depth of 10 microns.

Round anodes of 1.5 mm diameter and 45 mm length, embedded in cylindrical polypropylene holders of 5 mm diameter were used. They were prepared from 99999 copper rod (Comincon Cl., Spokane, Wash.). Polycrystalline specimens were used as received, or annealed (1750°F, 4 hrs. in argon, after 7.5% diameter reduction). Single crystals were grown from the same material in induction-heated graphite molds, using spherical seed crystals. The surfaces of the embedded electrodes were gently polished over extended periods (6-30 hrs.) with 1 and 0.5 micron chromium oxide abrasive. Structural damage due to this treatment was sufficiently shallow as not to be visible in the x-ray diffraction pattern of single crystals. In order to put a limit on the depth of lattice damage expected to be still present on the surface (without affecting the x-ray diffraction pattern), experiments were performed to determine the thickness of distorted copper necessary to obliterate the diffraction from an underlying single crystal. Cold-rolled copper foils of different thicknesses were attached to the surface of a (100) oriented crystal. No discernible diffraction pattern was obtained with a 10 micron thick foil and a greatly attenuated one resulted from 5 microns, independent of the closeness of contact of the copper foil. These results indicate that surface damage due to polishing, extended to a depth of much less than 5 microns, and the anodic dissolution indeed proceeded into the undisturbed crystal. The smoothness and flatness of the polished electrode surface was asserted by interference microscopy.

Deviation from flatness over the entire surface was usually less than 2 microns as illustrated in Fig. 2. Residual polishing marks were at most 0.05 micron deep (Fig. 3).

Before use, the electrodes were cleaned with acetone and detergent and subjected to cathodic hydrogen evolution in 1M NaOH (100 mA/cm^2, 3 min.). After the dissolution experiment, the electrodes were immediately removed from the flow channel cell, rinsed with distilled water and dried with acetone. Without delay, they were examined by optical microscopy and interference microscopy. From some surfaces, plastic-carbon replicas were prepared for transmission electron microscopy, others were examined in the scanning electron microscope.

Active Dissolution

Fig. 4 shows the surface of an annealed polycrystalline electrode after dissolution in the active mode. The exhibition of individual grains, similar to chemical etching, suggest that anodic attack depends on crystallographic orientation. The same surface viewed at higher magnification (Fig. 5) demonstrates that the different appearance of grains is due to the development of ridges and shallow etch pits, whose orientation and shape vary among adjacent grains. Still higher magnification reveals that ridges and etch pits are composed of submicroscopic steps (Fig. 6). These observations are similar to those reported from electrocrystallization and vaporization studies. They can be related to the mechanism of removal of atoms from the crystal lattice which can be described by the movement of atomic ledges across close packed lattice planes.

In order to investigate the effect of crystal orientation, experiments were also carried out with single crystal electrodes. Contrary to the

polycrystals which exhibited a dull appearance after active dissolution, single crystal surfaces of low index orientation remained bright without visible etching. This difference is illustrated in Fig. 7 which may be compared to Fig. 5 taken at the same magnification. The (110) face employed in Fig. 7 shows surface texture at the limit of optical resolution. On the (100) face, only the electron microscope revealed shallow crystallographic etch patterns and even at that resolution, the (111) face was almost featureless, as shown in Fig. 8. These results seem to support a dissolution mechanism involving the motion of monatomic ledges on tightly packed lattice planes.[6] These observations are also consistent with those of Hulett and Young[7] who found the formation of etch pits on (111) copper faces in HCl at low current densities only after the addition of HBr which acted as a poison for ledge motion. No such poisoning appears to have occurred under the present dissolution conditions. According to the ledge motion mechanism, dissolution starting with a high index crystal plane, (comparable to the random orientation of grains in polycrystalline material) is expected to result in a faceted surface. Such facets have been observed on several randomly oriented crystals. A typical example is shown in Fig. 9. This surface texture is similar to the one reported for iron cathodically deposited at high (150-200 mV) overvoltage.[8] The surface textures resulting from active dissolution indicate that dissolution at very high rates does not proceed by a basically different mechanism from that at low rates, provided that removal of reaction products from the surface by convective diffusion and migration is sufficiently fast.

Transpassive Dissolution

Fig. 10 illustrates a polycrystalline surface after transpassive dissolution. In contrast to the appearance of the same specimen after active dissolution (Fig. 4), the surface now is bright and differences between individual grains are barely discernible at the optical level of resolution. A large number of round, deep pits, some arranged in rows, is distributed over the surface. Streaks in the flow direction, due to a waviness of the surface, extend from the leading edge over most of the specimen. Bright and pitted surfaces, resulting from dissolution in the presence of an anodic passivating layer, have also been reported for electropolishing at much lower current densities.[9] Brightness is due to a greatly reduced micro-roughness, and the even attack on differently oriented grains has been explained by the equalizing effect of an oxide layer.[10] At much higher resolution, differences in surface texture between neighboring grains occasionally become visible. The electron micrograph, Fig. 11, illustrates one of the most pronounced microtextures observed after transpassive dissolution. Compared to the surface resulting from active dissolution shown in Fig. 6 at the same magnification, the roughness is an order of magnitude lower.

The difference in microtexture between active and transpassive dissolution is particularly pronounced with a randomly oriented single crystal. The electron micrographs in Fig.12 illustrate this situation for a surface oriented 10° off the (110) plane. Interestingly enough, no pitting has been observed on any of the single crystals studied. Flow streaks appeared on single crystals in transpassive dissolution similar to the ones observed on polycrystalline specimen. The interferogram, Fig. 13,

shows the associated macroscopic waviness of the surface. Typically these profiles are 0.1 mm wide, a few microns deep, and become shallower and wider downstream. Flow streaks observed under technical ECM conditions have been attributed to cavitation effects. In the present study, flow streaks have not been observed in active dissolution, where cavitation is more likely, due to the higher flow rates. (2500 cm/sec active, 400 cm/sec transpassive).

Conclusions

1. The present study shows that crystallographic factors influence the surface texture resulting from high-rate anodic dissolution of copper in the active mode. Transpassive dissolution proceeds in the presence of anodic layers, which diminish the effect of crystal orientation and lead to brightening.
2. In the active mode, submicroscopic facets lead to the development of ridges, which give the surface an etched appearance. This appearance depends on crystallographic orientation and results in a differentiation between grains in polycrystalline material. Active dissolution of (100) and (111) faces has not resulted in the formation of facets. These observations are in agreement with a dissolution mechanism based on the motion of atomic ledges on tightly packed lattice planes.
3. Flow streaks are associated with transpassive dissolution, while the surface resulting from active dissolution is independent of flow direction.
4. Transpassive pitting is linked to metallurgical factors not present in the single crystals studied.

Acknowledgment: The authors wish to thank Mr. W. T. Giba for the preparation of electron microscope replica and other valuable assistance in this investigation. This work was conducted under the auspices of the U. S. Atomic Energy Commission.

References

1. D. Landolt, R. H. Muller and C. W. Tobias, J. Electrochem. Soc. 116, 1384 (1969).
2. D. Landolt, R. Acosta, R. H. Muller and C. W. Tobias, J. Electrochem. Soc. 117, 839 (1970).
3. K. Kinoshita, D. Landolt, R. H. Muller and C. W. Tobias, J. Electrochem. Soc. 117, 1246 (1970).
4. J. O'M. Bockris and G. A. Razumney, Fundamental Aspects of Electrocrystallization, Plenum Press, New York, 1967.
5. R. W. Mar and A. W. Searcy, J. Chem. Phys., in press.
6. R. Kaischew and E. Budevski, Contemp. Phys. 8, 489 (1967).
7. L. D. Hulett, Jr., and F. W. Young, Jr., J. Phys. Chem. Solids 26, 1287 (1965).
8. K. E. Heusler and R. Knoedler, Electrochim. Acta 15, 243 (1970).
9. T. P. Hoar, G. P. Rothwell, Electrochim. Acta 9, 135 (1964).
10. T. P. Hoar, Corros. Sci. 7, 341 (1967).
11. T. P. Hoar, D. C. Mears, G. P. Rothwell, Corros. Sci. 5, 279 (1965).
12. J. Bayer, M. A. Cummings, H. V. Jollis, TID Report ML TDR 64313, General Electric Co. (1964).
13. R. R. Cole, Y. Hopenfeld, Trans. ASME (B) 85, 395 (1963).
14. S. Maeda, N. Saito and S. Arai, Technical Report, Nagoya Works, Mitsubishi Electric Corp., Aug. 1963.

Figure Captions

Fig. 1. Polycrystalline copper surfaces after dissolution in 2 M KNO_3 at different current densities and flow velocities. Optical micrographs.

Fig. 2. Low power interference micrograph of polished copper single crystal electrode surface 10° off (110) orientation. Maximum deviation from flatness, 2 microns.

Fig. 3. High power interference micrograph of polished copper single crystal electrode surface 10° off (110) orientation. Maximum depth of residual polishing marks 0.05 microns.

Fig. 4. Differentiation of grains in annealed polycrystalline copper after active dissolution. Optical micrograph.

Fig. 5. Ridges and etch pits on different grains after active dissolution. Same specimen as in Fig. 4.

Fig. 6. Submicroscopic steps in a grain of polycrystalline copper after active dissolution. Electron micrograph of two-stage carbon replica. Diameter of latex spheres 0.5 micron.

Fig. 7. (110) single crystal surface with barely visible texture after active dissolution. Optical micrograph.

Fig. 8. Smooth copper (111) surface after active dissolution. Latex sphere of 0.53 μ diameter provides scale for direction and length of shadows. Electron micrograph of two-stage carbon replica.

Fig. 9. Copper single crystal surface, oriented 10° off (110) direction after active dissolution. Scanning electron micrograph, tilted 30°.

Fig. 10. Bright, pitted surface with flow streaks. Annealed polycrystalline copper after transpassive dissolution. Optical micrograph. Flow direction from lower left to upper right.

Fig. 11. Surface texture of neighboring grains of annealed, fine grain polycrystalline copper after transpassive dissolution. Electron micrograph of two-stage carbon replica.

Fig. 12. Microtexture of copper single crystal oriented 10° off (110) (a) after active dissolution, (b) after transpassive dissolution, same magnification. Electron micrographs of two-stage carbon replicas, diameter of latex spheres 0.53 micron.

Fig. 13. Flow streaks resulting from transpassive dissolution of (100) single crystal face. Interference micrograph. Flow direction from left to right.

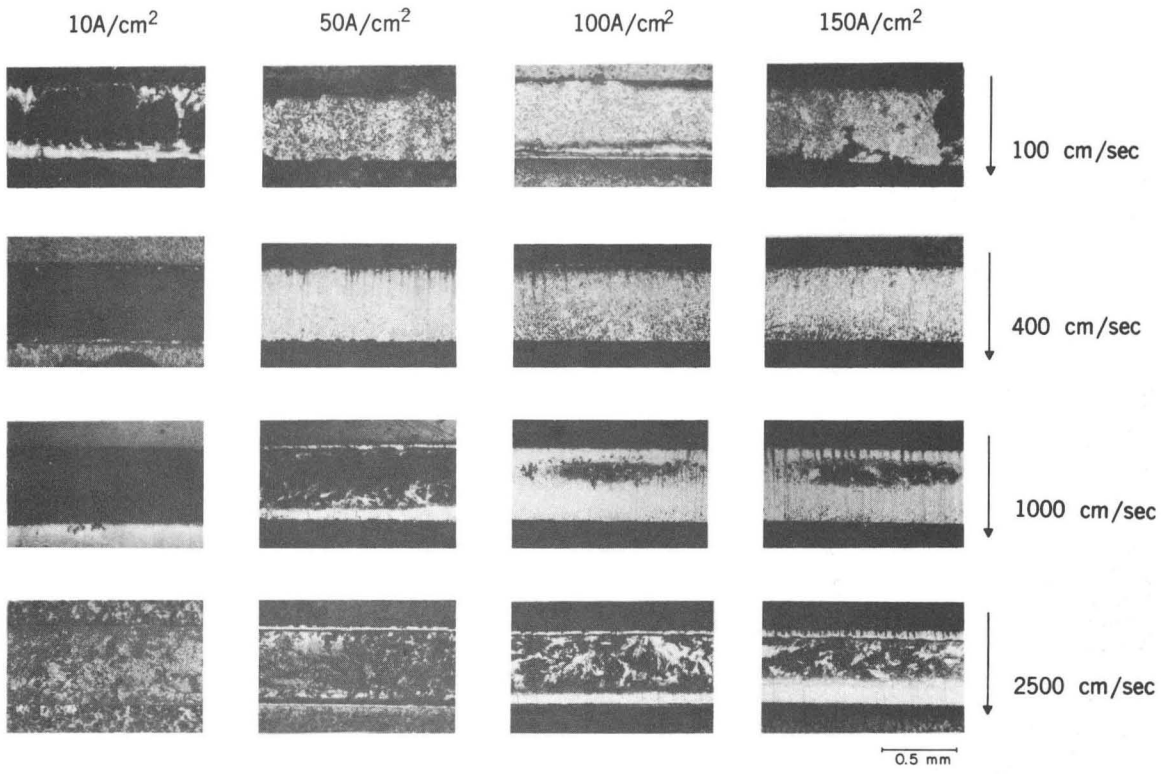

COPPER DISSOLUTION IN 2N KNO_3 AT CONSTANT CURRENT

XBB681-205

Fig. 1.

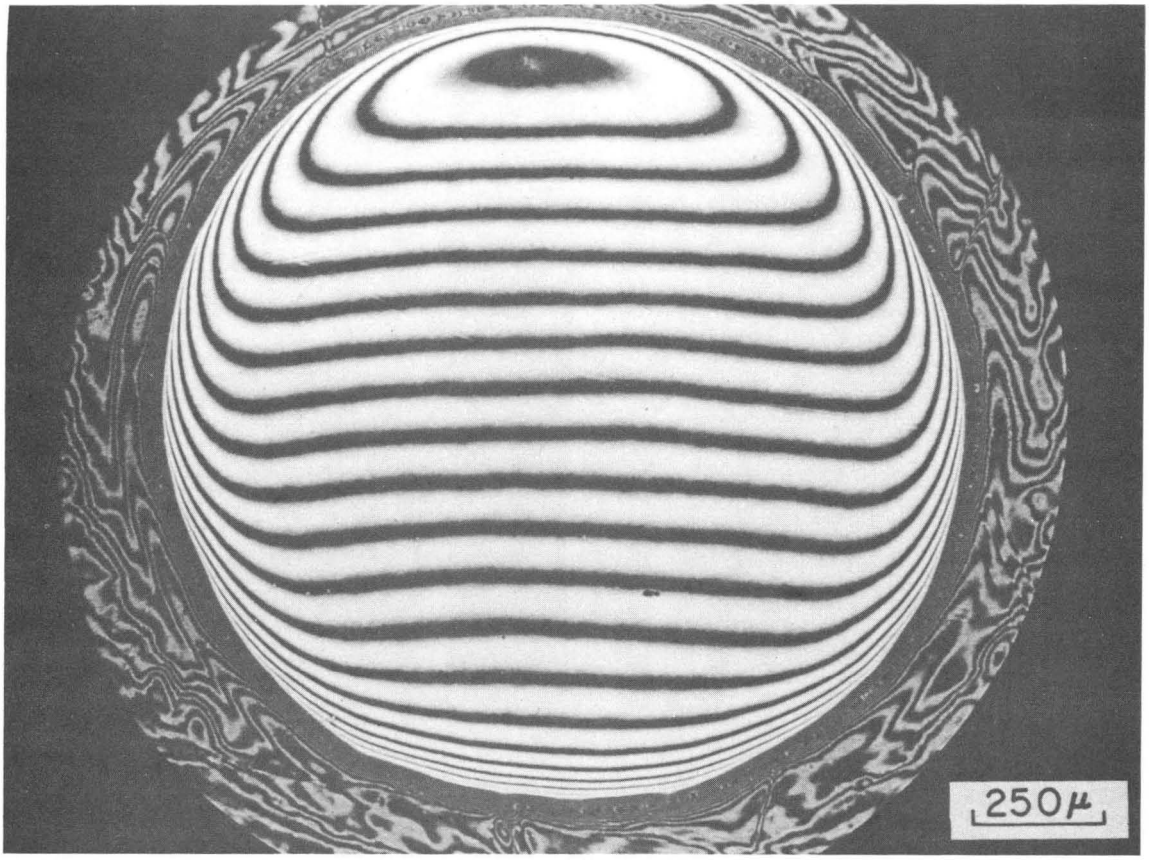

XBB709-3975A

Fig. 2.

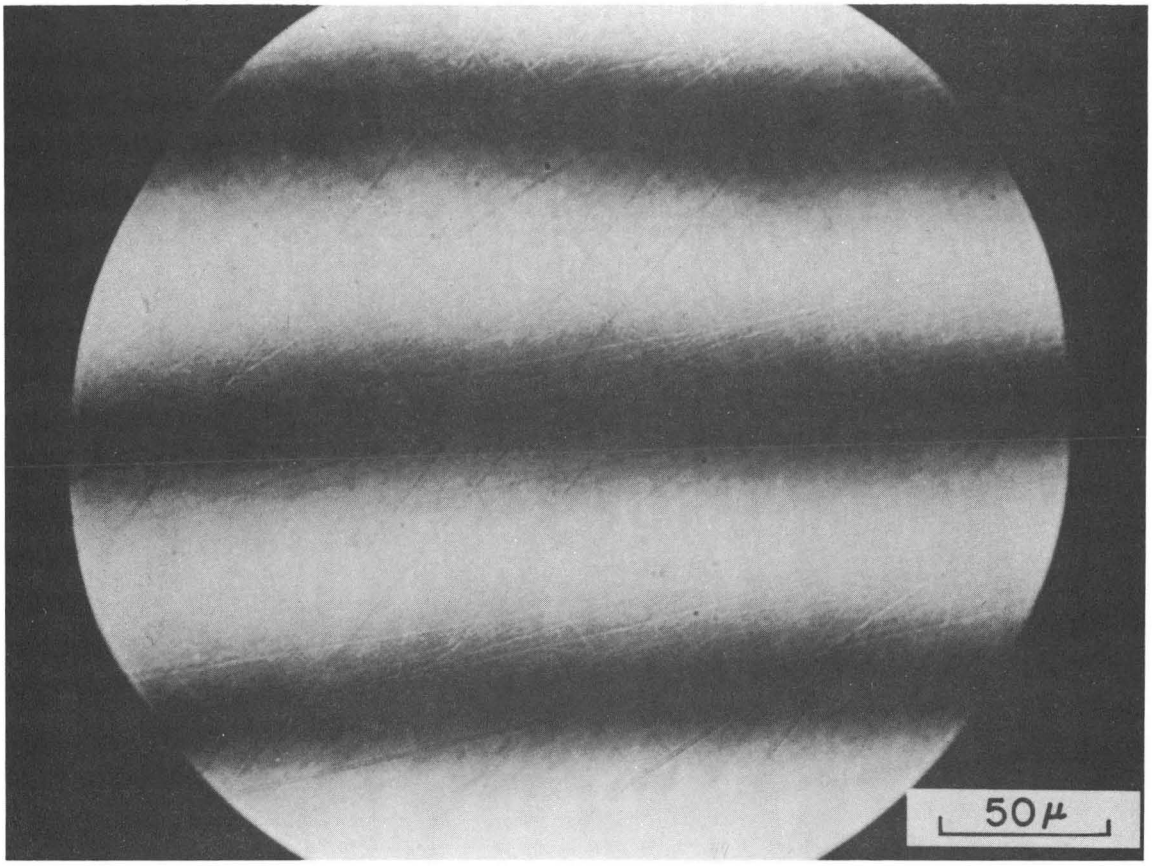

XBB709-3976A

Fig. 3.

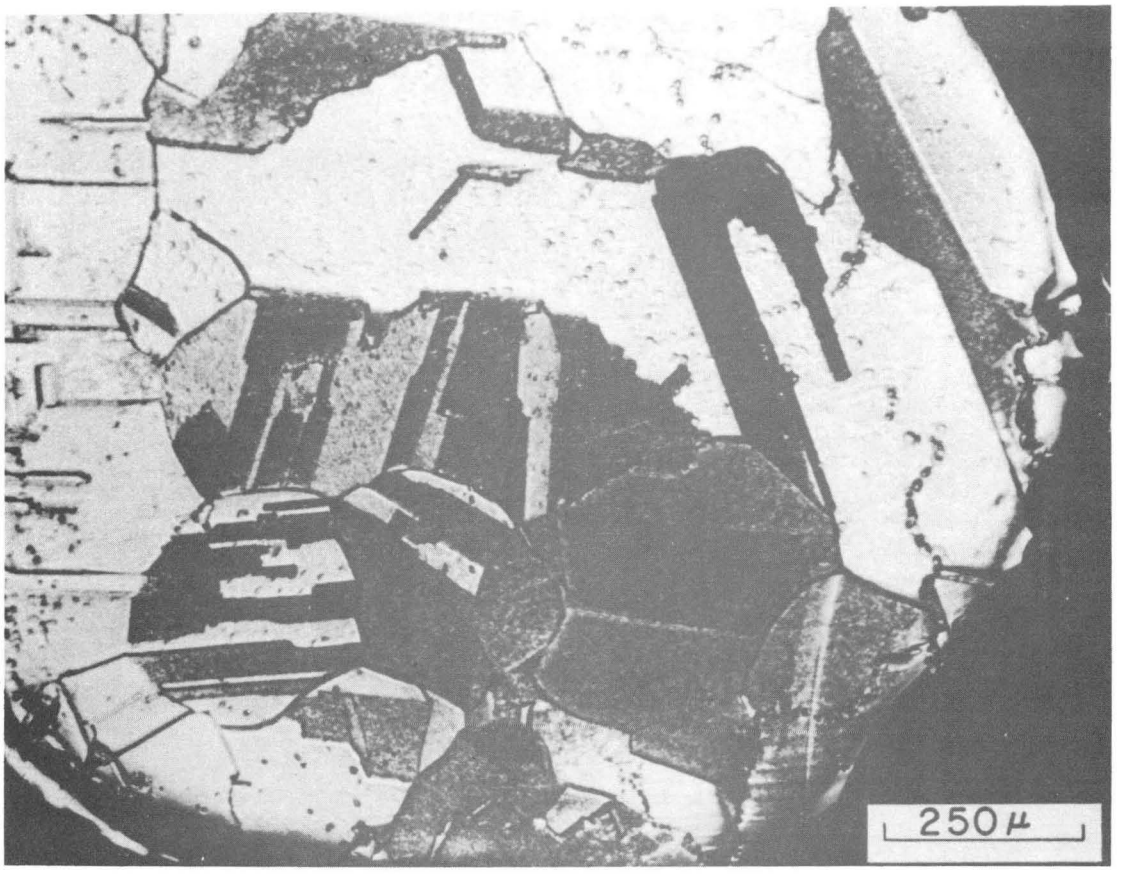

XBB709-3964A

Fig. 4.

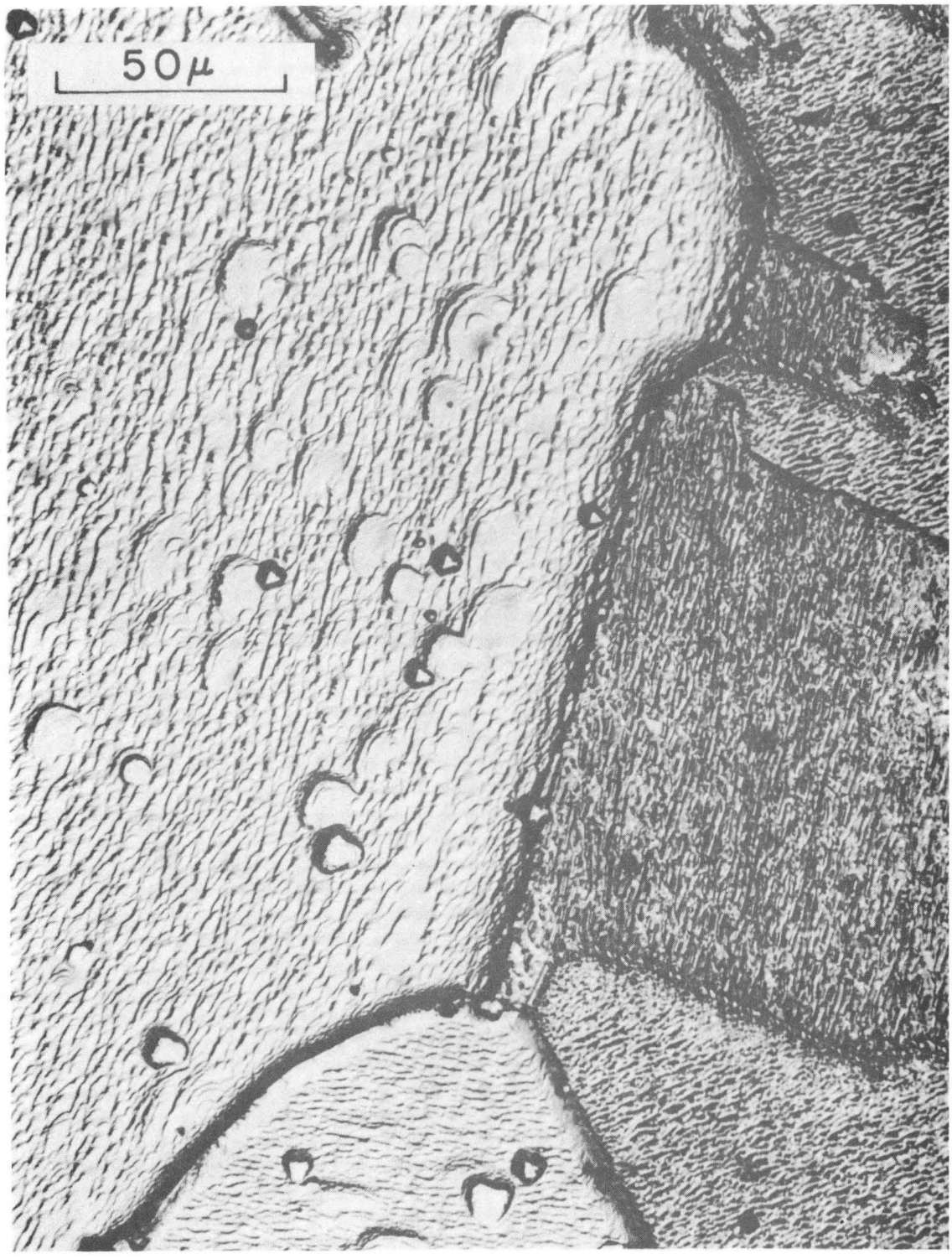

XBB709-3974A

Fig. 5.

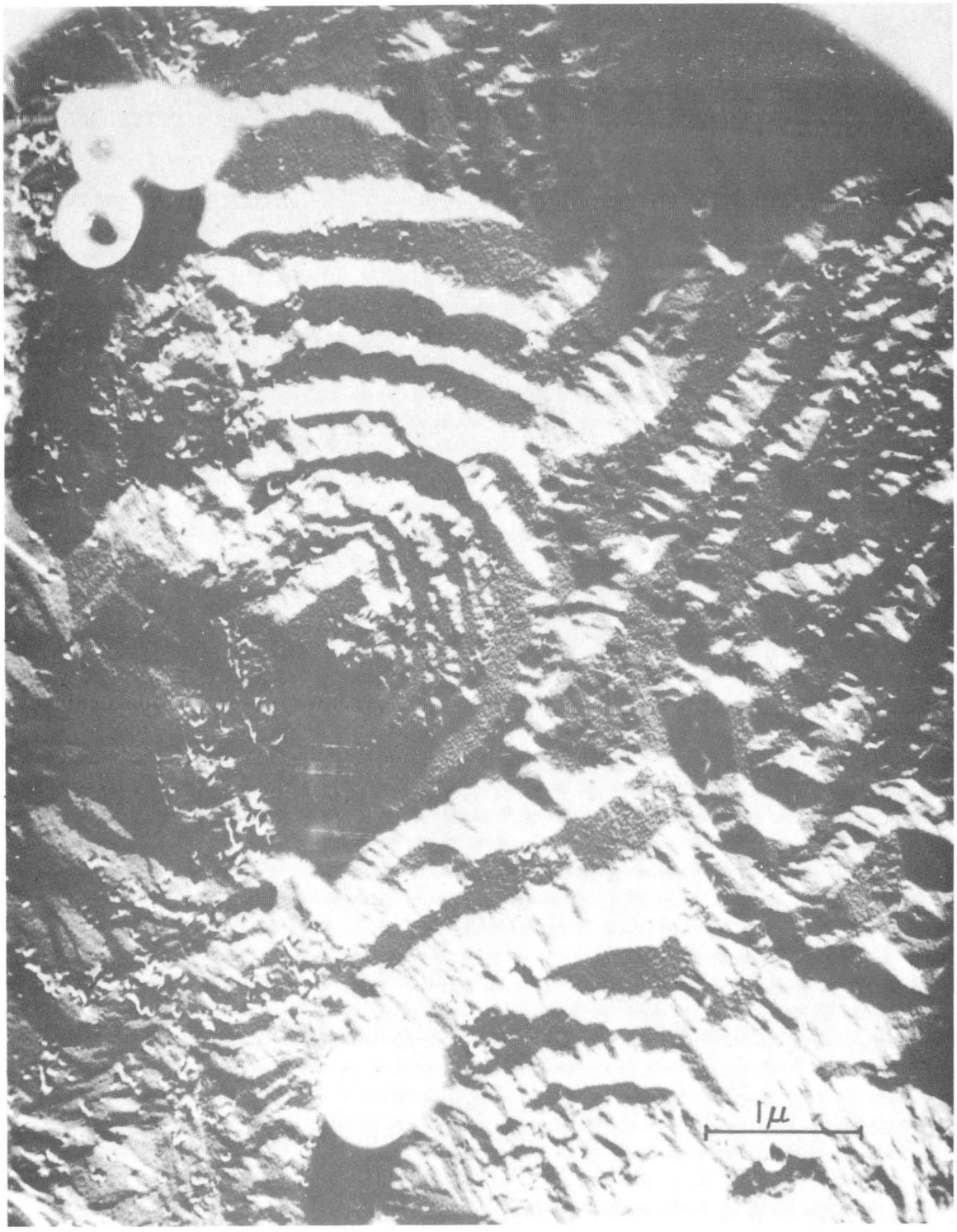

XBB709-4045

Fig. 6.

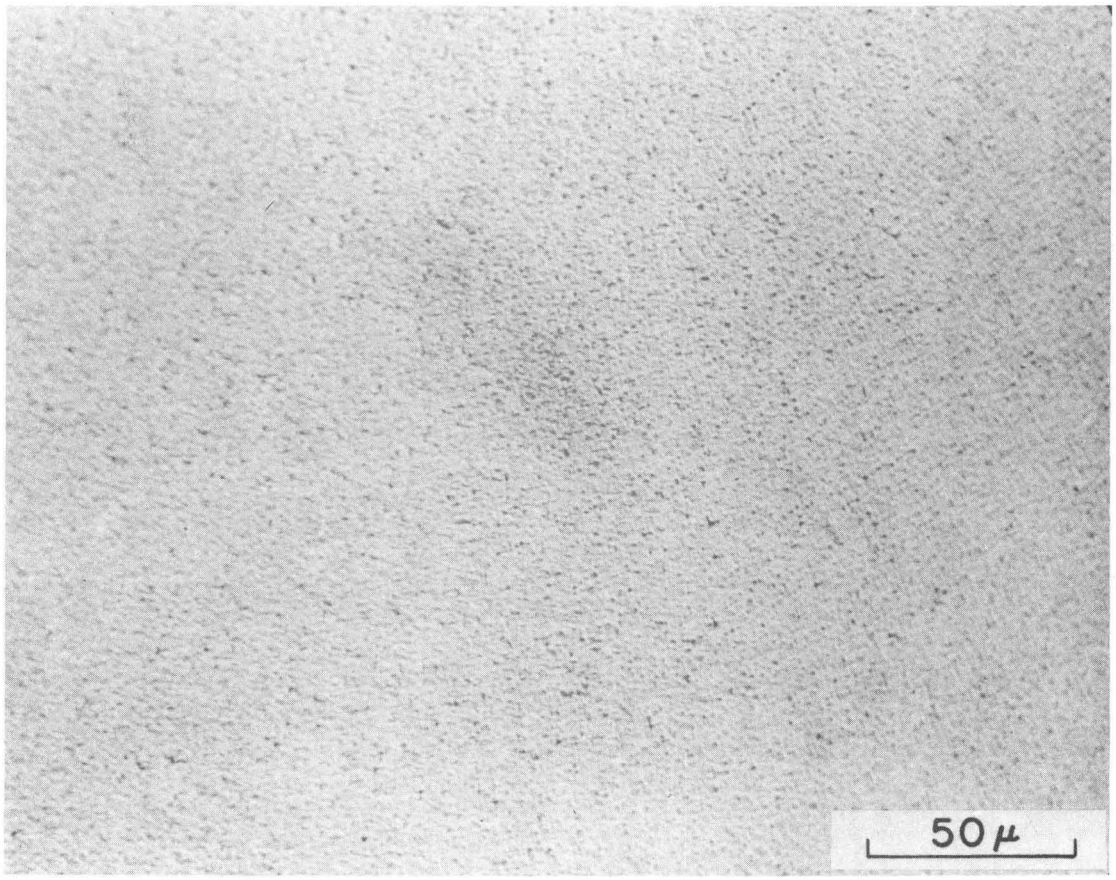

XBB709-3965A

Fig. 7.

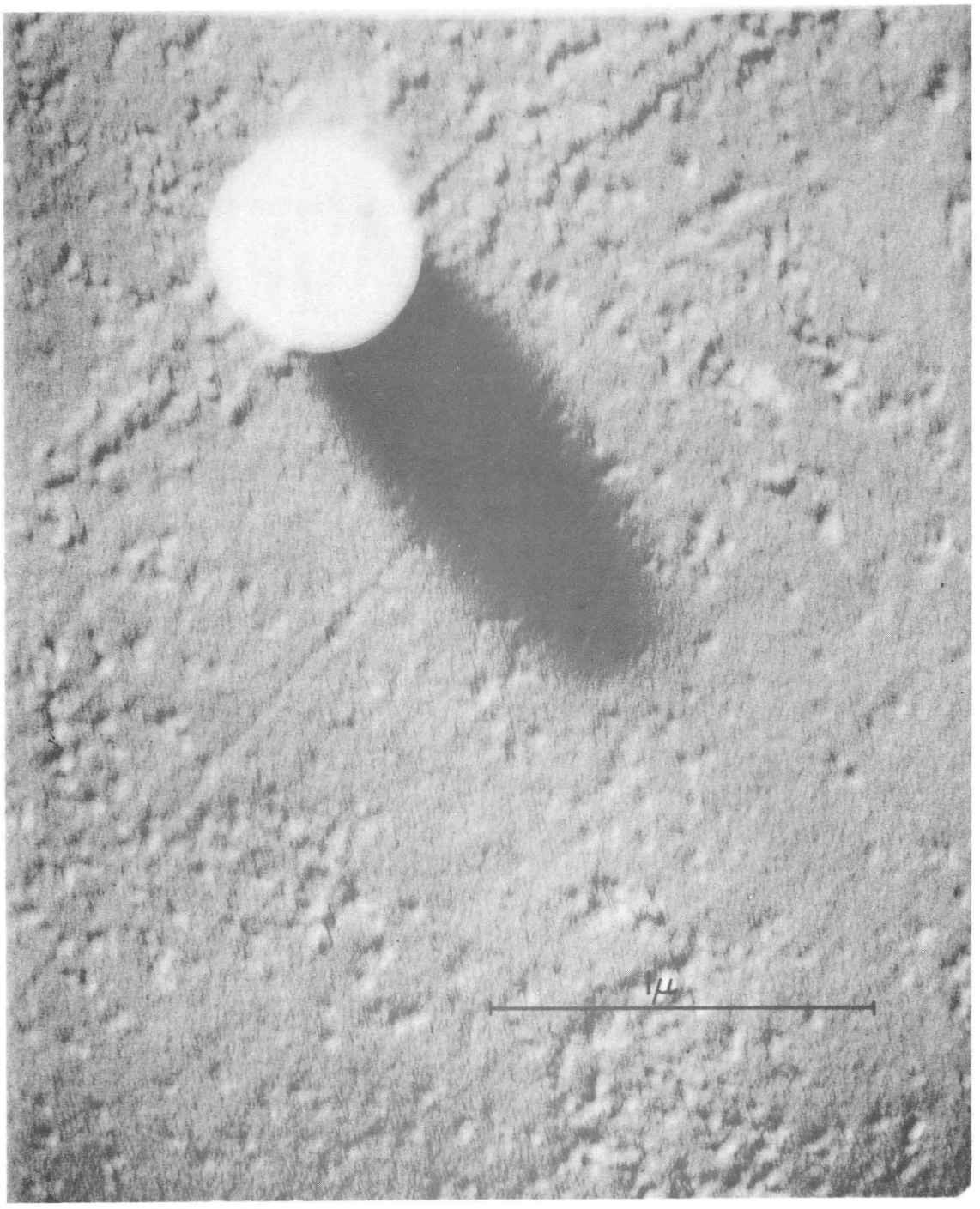

XBB709-4043

Fig. 8.

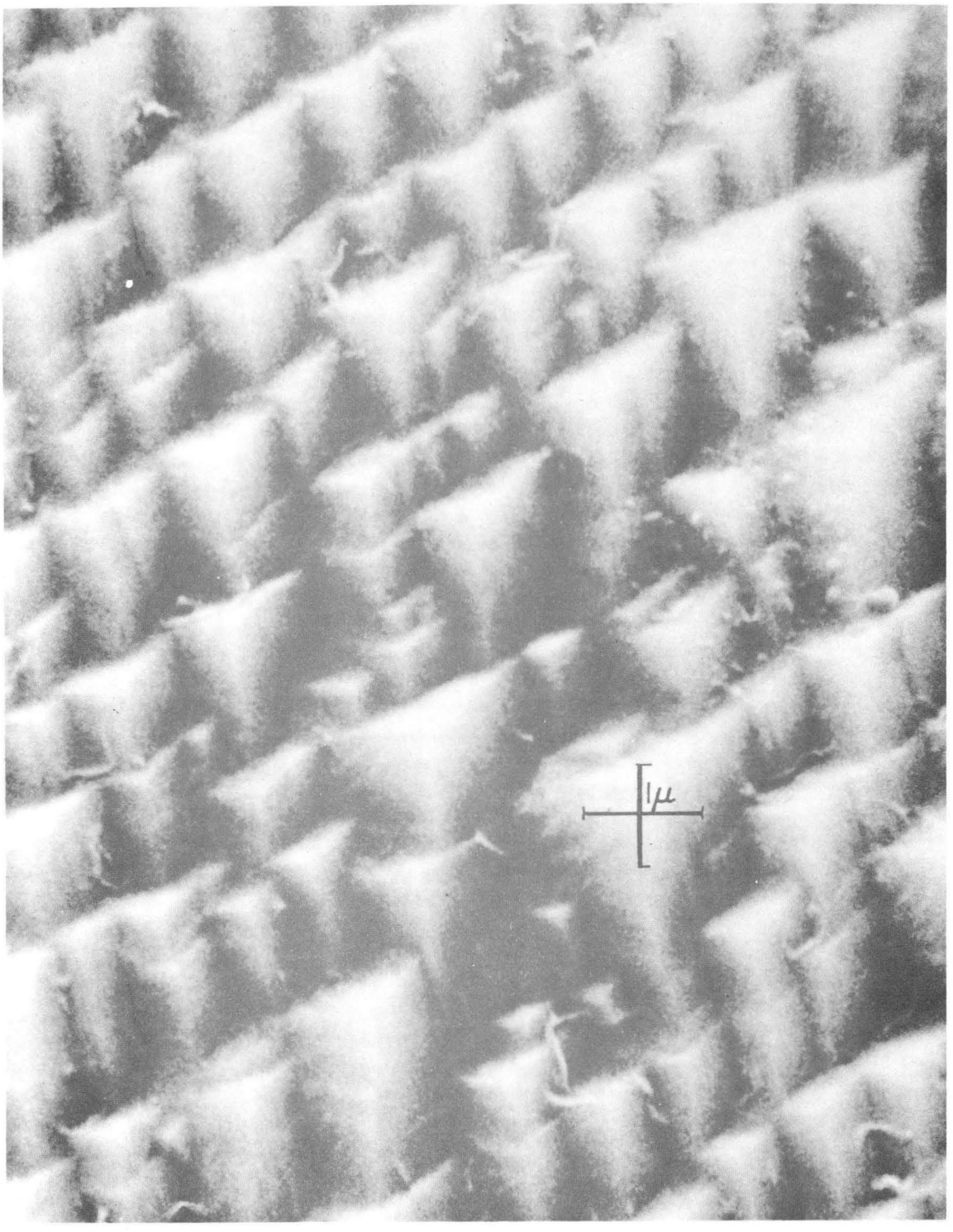

XBB709-4046

Fig. 9.

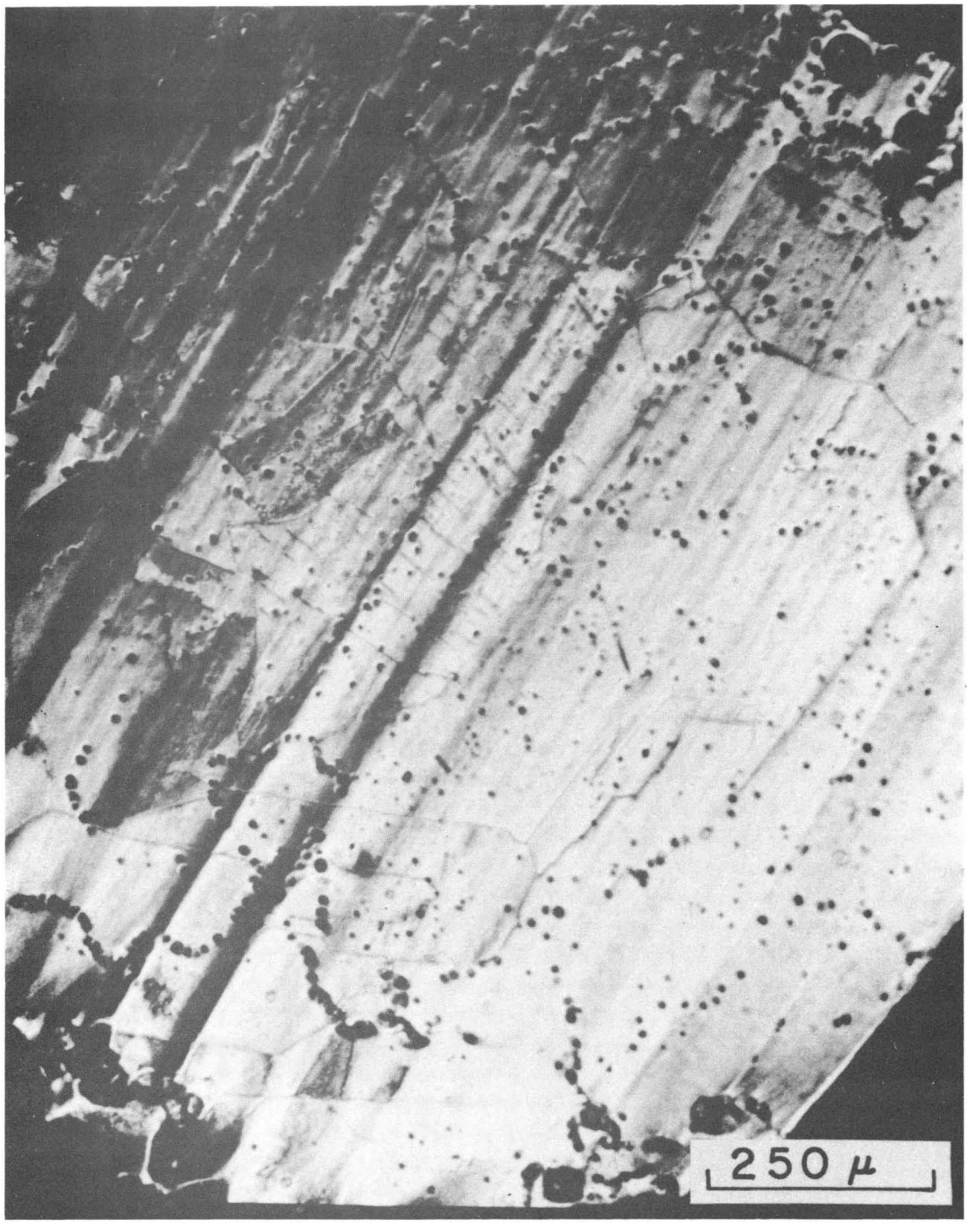

XBB709-3963A

Fig. 10.

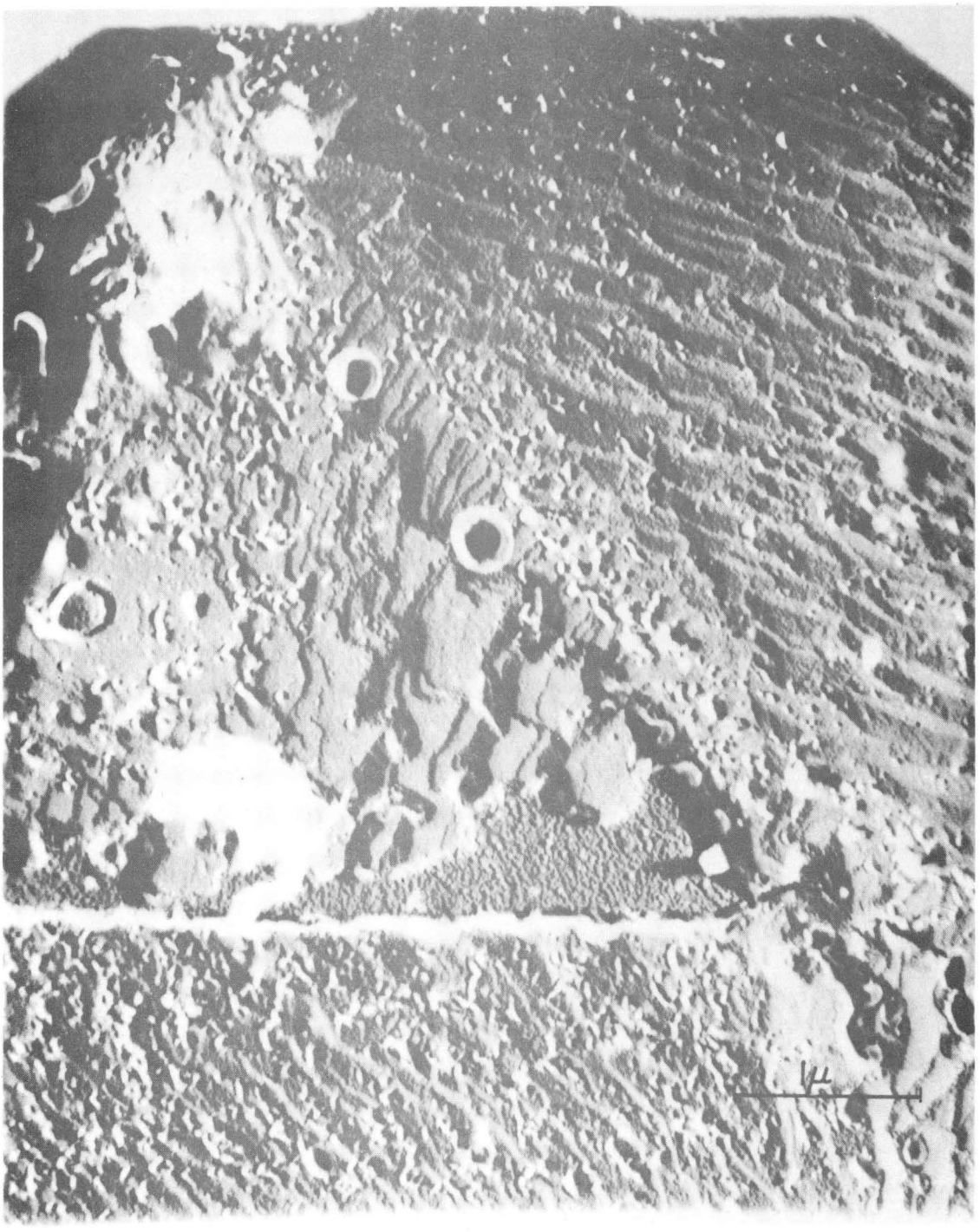

XBB709-4044

Fig. 11.

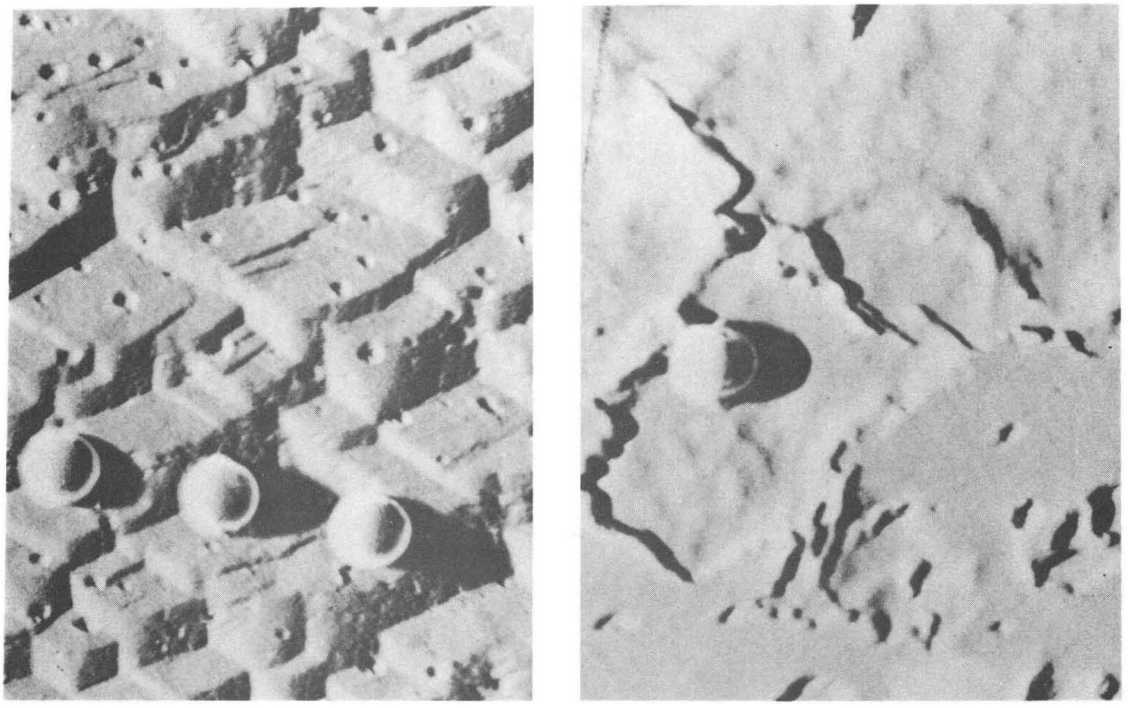

(a) (b)

XBB709-4175

Fig. 12.

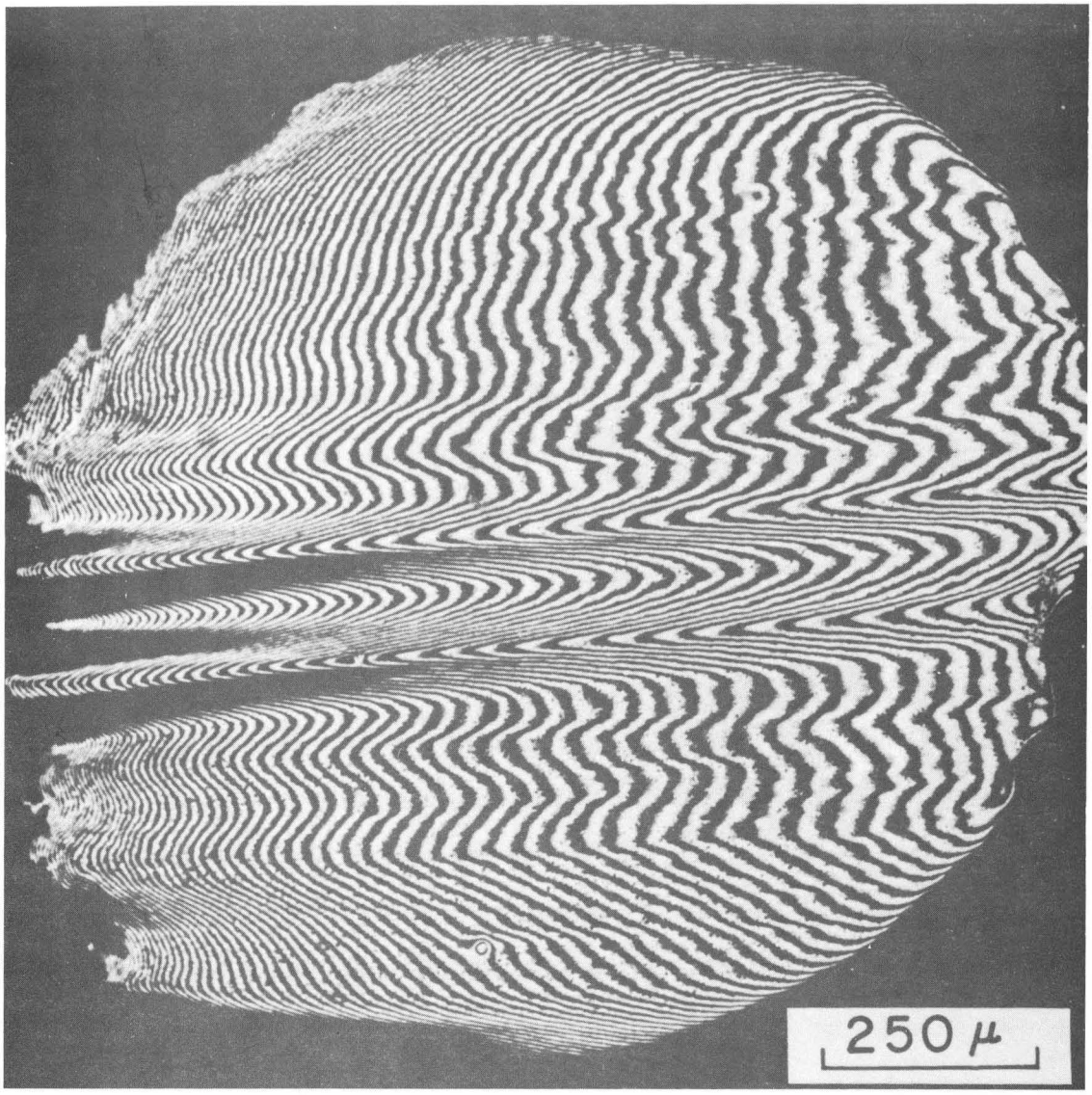

XBB702-962A

Fig. 13.

LEGAL NOTICE

This report was prepared as an account of Government sponsored work. Neither the United States, nor the Commission, nor any person acting on behalf of the Commission:

A. Makes any warranty or representation, expressed or implied, with respect to the accuracy, completeness, or usefulness of the information contained in this report, or that the use of any information, apparatus, method, or process disclosed in this report may not infringe privately owned rights; or

B. Assumes any liabilities with respect to the use of, or for damages resulting from the use of any information, apparatus, method, or process disclosed in this report.

As used in the above, "person acting on behalf of the Commission" includes any employee or contractor of the Commission, or employee of such contractor, to the extent that such employee or contractor of the Commission, or employee of such contractor prepares, disseminates, or provides access to, any information pursuant to his employment or contract with the Commission, or his employment with such contractor.

TECHNICAL INFORMATION DIVISION
LAWRENCE RADIATION LABORATORY
UNIVERSITY OF CALIFORNIA
BERKELEY, CALIFORNIA 94720